

01000011 01101000 01100001 01110000
01110100 01100101 01110010 00100000
00110010 00101110 00110101 00001010

Chapter 2.5

The anatomical relationship of the superficial radial nerve and the lateral antebrachial cutaneous nerve: A possible factor in persistent neuropathic pain.

A.R. Poublon, E.T. Walbeehm, L.S. Duraku, P.H.C. Eijlers, A.L.A. Kerver, G.J. Kleinrensink, J.H. Coert.

J Plast Reconstr Aesthet Surg. 2014 Oct 16.

ABSTRACT

Background: The superficial branch of the radial nerve (SBRN) is known for developing neuropathic pain syndromes after trauma. These pain syndromes can be hard to treat due to the involvement of other nerves in the forearm. When a nerve is cut, the Schwann cells, and also other cells in the distal segment of the transected nerve, produce the nerve growth factor (NGF) in the entire distal segment. If two nerves overlap anatomically, similar to the lateral antebrachial cutaneous nerve (LACN) and SBRN, the increase in secretion of NGF, which is mediated by the injured nerve, results in binding to the high-affinity NGF receptor, tyrosine kinase A (TrkA). This in turn leads to possible sprouting and morphological changes of uninjured fibers, which ultimately causes neuropathic pain. The aim of this study was to map the level of overlap between the SBRN and LACN.

Methods: Twenty arms (five left and 15 right) were thoroughly dissected. Using a new analysis tool called CASAM (Computer Assisted Surgical Anatomy Mapping), the course of the SBRN and LACN could be compared visually. The distance between both nerves was measured at 5-mm increments, and the number of times they intersected was documented.

Results: In 81% of measurements, the distance between the nerves was >10 mm, and in 49% the distance was even <5 mm. In 95% of the dissected arms, the SBRN and LACN intersected. On average, they intersected 2.25 times.

Conclusions: The close (anatomical) relationship between the LACN and the SBRN can be seen as a factor in the explanation of persistent neuropathic pain in patients with traumatic or iatrogenic lesion of the SBRN or the LACN.

INTRODUCTION

In 1984, Dellon and Mackinnon¹ stated that surgery on the radial side of the wrist is notorious for the development of neuropathic pain. Their explanation was that in 80% of cases the cause of this complication was stretching or compression of the superficial branch of the radial nerve (SBRN).

Mackinnon and Dellon² also presumed that the persisting symptoms in some patients might be caused by the fact that the course of the lateral antebrachial cutaneous nerve (LACN) for a large part overlaps with the course of the SBRN. Thus, when the SBRN is lacerated, the LACN almost certainly also is cut. Therefore, they postulated that in these patients the pain was caused by the LACN and not the SBRN.

By performing a diagnostic nerve block to the LACN using a local anesthetic (1% lignocaine), pain can be temporarily reduced in some patients³ This shows that there is at least a relation between pain caused by lesion of the radial superficial nerve (SBRN) and the LACN. However, it remains unclear at which level the actual problem is localized: the distal segment, the dorsal root ganglion (DRG), or even central parts of the nervous system.⁴

It has been postulated that the nerve growth factor (NGF) plays a role in neuropathic pain,⁵⁻⁸ although the exact mechanisms remain elusive.^{9,10} When a nerve is transected, Schwann cells, but also other cells, in the entire distal segment of this transected nerve produce NGF^{11,12} This production is initiated by axonal degeneration and Schwann cell upregulation, also known as Wallerian degeneration. If the branches of two nerves overlap anatomically (e.g., in the case of the LACN and SBRN), the produced NGF in the distal part of one nerve stimulates the other nerve, causing pain. Therefore, our interest is to demonstrate the areas of overlap between the LACN and SBRN more precisely. This is hard to describe by standard anatomical techniques and, therefore, a system called Computer Assisted Surgical Anatomy Mapping (CASAM) was used. CASAM is a system created in the Erasmus MC Anatomy laboratory^{13,14} that can create an average of all used dissections (i.e., a virtual “average arm”) and subsequently create a visual representation of the “average” course of the SBRN and the LACN (see the CASAM section below).

The goals of the study were twofold: to describe the variation in the anatomy of the LACN and the SBRN, and to quantify the amount of overlap between the LACN and the SBRN by creating a visual model using CASAM.

METHODS

Materials

Twenty arms (nine male and 11 female; mean age 79.35 years (range 61–90); 15 right and five left) were embalmed with a solution containing 4% formalin preceded by flushing the specimen with Anubifix™. All dissections were performed using a 2.5× magnifying loupe.

To ensure comparable exposures, the dissection and imaging method were standardized.¹⁴ Incisions were made from 5 cm below the caput humeri up to 5 cm above the elbow exposing the biceps. At the ends of the incision lines, two perpendicular incisions were made, creating two skin flaps that could be removed laterally and medially. Once the biceps brachi muscle was exposed, the fascia surrounding the muscle was incised and via blunt preparation the biceps was released from the underlying muscle tissue. Right behind the biceps, the musculocutaneous nerve, being the origin of the LACN, could be identified and the biceps was cut at the insertion and removed proximally. The LACN was dissected along its course distally down to the metacarpal region. Along the way, the nerve was marked using colored pins. Once the distal one-third of the arm was reached, the brachioradialis (BR) muscle was identified and bluntly dissected from the underlying tissue, while keeping the LACN intact.

In step 2, the SBRN was identified deep to the BR muscle. Once identified, the nerve was followed to the insertion of the BR where it continued to run a more superficial course. This spot was also marked with a colored pin. The SBRN was also dissected distally down to the metacarpal joint level.

Measurements

To quantify our findings, necessary to operate CASAM, the following measurements were taken:

- 1) The distance between both the epicondyles and the point where the SBRN emerges
- 2) The distance to both epicondyles and the first branch of the SBRN (the same procedure was performed with regard to the LACN)
- 3) The distance between both epicondyles and the location of crossings between the SBRN and LACN

Furthermore, along the course of both nerves, every 5 mm, the smallest distance between the SBRN and the LACN was measured using digital calipers (IP67 waterproof digital caliper, Hogetex, Varsseveld, the Netherlands).

Every arm was photographed with a digital camera (Nikon D 60 with Sigma 50 mm 1:2,8 DG MACRO lens). The camera was placed perpendicular to the specimen at a distance of 100 cm on a tripod. The pictures were loaded onto Photoshop CS4, and the measurements performed on each arm were stored digitally.

Computer-Assisted Surgical Anatomy Mapping (CASAM)

As human arms vary in size, anatomical comparison can be difficult. Therefore, a program called CASAM was used. In CASAM, it is possible to morph the digital image of each individual arm to the average size of all arms.

CASAM is based on the fact that “bony landmarks” (BLs), such as Lister’s tubercle, lie in the same place relative to every arm. Besides BLs, the so-called shape-defining landmarks (SDLs) were created, to mark the outline of the arm, by dividing the space between two BLs into equal parts. We take these BLs and SDLs and mark them in the program. The picture can now be warped around these bony landmarks using active shape modeling (ASM) creating an average arm. All arms are then warped to the dimensions of the average arm, making it possible to compare all the arms directly. The “scaled” course of the SBRN and the LACN of all individual arms can now be compared directly.

The “bony” landmarks were used at: the lateral and medial epicondyle, the caput ulnae, Lister’s tubercle, the lateral and the medial side of the metacarpophalangeal (MCP) and interphalangeal (IP) joints of the thumb, the caput phalanx I of the index finger, and the caput phalanx I of the third finger (Figure 1, green marks). These BLs were used, because their relative position in each arm is the same. The distance between the epicondyles and caput ulnae was divided into four equal parts, thus forming the three SDLs at the dorsal site of the arm. At the ventral side of the arm, the distance between the medial epicondyle and MCP I was divided into four equal parts, forming the ventral SDLs. The last two SDLs were defined as follows: halfway between the medial and lateral epicondyle and halfway between the caput ulnae and caput phalanx I (Figure 1, blue marks.)

The image created by CASAM shows a template of the individual course of the SBRN and the LACN, scaled to the average dimension of all 20 arms. The mean distance between a line through the lateral and medial epicondyle and Lister’s tubercle was 239.15 mm (range 209–281 mm). This distance was used as the reference length of the arm.

Photoshop CS4 was used to trace the SBRN and the LACN in all pictures of the specimen. Then all morphed pictures could be compiled into one picture for further reference.

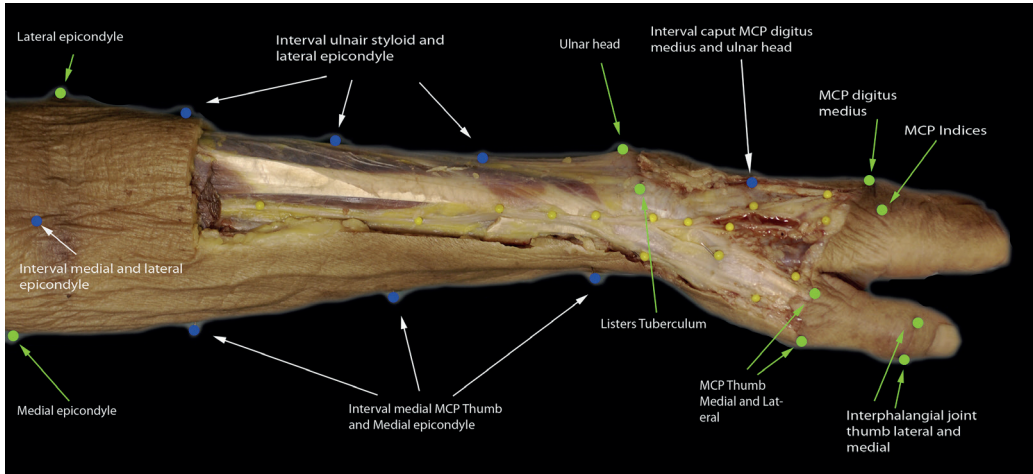


Figure 1. Landmarks used to outline the arm.

RESULTS

Topographic Anatomy

The LACN runs a course from a point under the biceps on the lateral side of the tendon in the elbow. It can be found in the subcutaneous fatty tissue on the radial side of the arm over the complete length of the forearm. It was noted that in 25% ($n = 5$) of cases the LACN branched early into two main branches continuing on both sides of the cephalic vein. In 70% ($n = 14$) of cases, the main branch of the LACN was localized volar to the cephalic vein. In 5% ($n = 1$) of cases, the LACN lay dorsal to the cephalic vein.

The radial nerve divides into the posterior interosseous nerve (PIN) and the SBRN emerging from a point deep to the BR muscle at an average distance of 159.6 mm (14.07) from the lateral epicondyle representing two-thirds of the length of the arm. On average, the SBRN showed 5.75 (five to seven) branches. Two branches reached the thumb, two reached the index finger, and one is localized in the direction of the middle finger. The SBRN was present in the subcutaneous fat tissue in the distal one-third of the arm.

In five arms, the SBRN and the LACN showed a total overlap, and in 14 arms partial overlap was observed. One arm showed no overlap ([Table 1](#)).

Nr	Left/ right	Gender	length of arm	SBRN branches	LACN branches	Crossings	overlap	LACN conjoins with WBRN
1	R	F	306	5	4	2	Yes	No
2	R	M	378	7	2	2	Yes	No
3	R	F	294	5	2	5	Yes	No
4	R	F	327	6	3	2	Yes	No
5	R	M	362	5	2	2	Yes	No
6	L	M	361	6	3	3	Yes	No
7	L	F	327	6	3	2	Yes	No
8	L	M	307	5	2	2	Yes	No
9	L	F	311	5	3	3	Yes	No
10	l	F	328	6	2	3	Yes	Yes
11	R	M	330	7	1	2	Yes	Yes
12	R	F	340	6	3	3	Yes	No
13	R	M	395	6	4	3	Yes	No
14	R	F	320	5	2	2	Yes	No
15	R	F	337	5	2	0	No	No
16	R	M	374	6	4	2	Yes	No
17	R	F	300	5	2	2	Yes	Yes
18	R	M	369	5	3	3	Yes	No
19	R	M	352	5	2	1	Yes	No
20	R	M	307	6	3	1	Yes	No

Table 1. Results of 20 arms.

In all cases, the main branch of the LACN runs volar to the point where the SBRN emerges. In the distal third of the arm where the two nerves overlap, the LACN crossed the SBRN with a mean of 2.25 times; these crossings ($n = 45$) occurred between 148.12 and 256.04 mm (corrected for length of the arm) distal to the lateral epicondyle. In 95% of the arms ($n = 19$), the LACN intersected with the SBRN at the point where the SBRN emerged from under the BR ([Figure 2](#)). A Pearson correlation of 0.820 with a significance of 0.00 (two-tailed) was found.

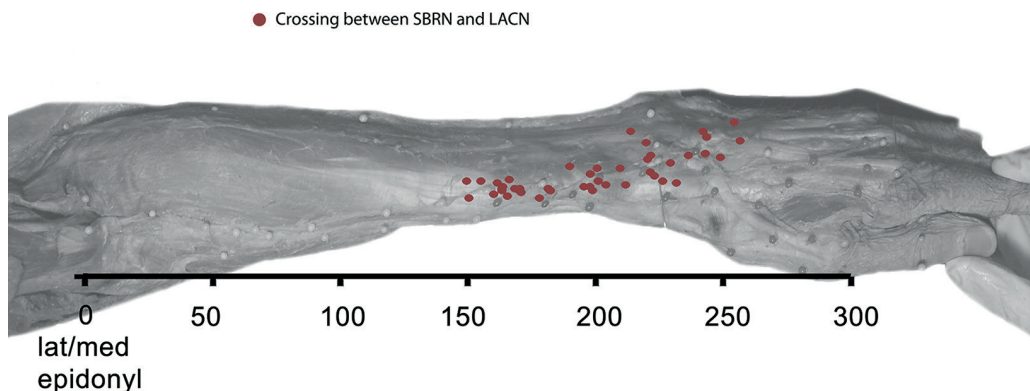


Figure 2. Spread of the intersection of the SBRN and LACN (corrected for length of the forearm).

Corrected for the length of the arm, the correlation coefficient dropped to 0.034, suggesting that there is an absolute distance between the two measurements. The distance between the first intersection and the site where the SBRN emerged from under the BR is 8.8 mm (standard deviation (SD) 12 mm). The distance between the nerves was measured in 5-mm intervals resulting in an average of 30 data points per arm. In 81% of the measurements, the distance between the two nerves was >10 mm and in 49% even lesser than 5 mm. In addition, the data show that the closest proximity can be found just after the SBRN emerges from under the deep fascia (Figure 3).

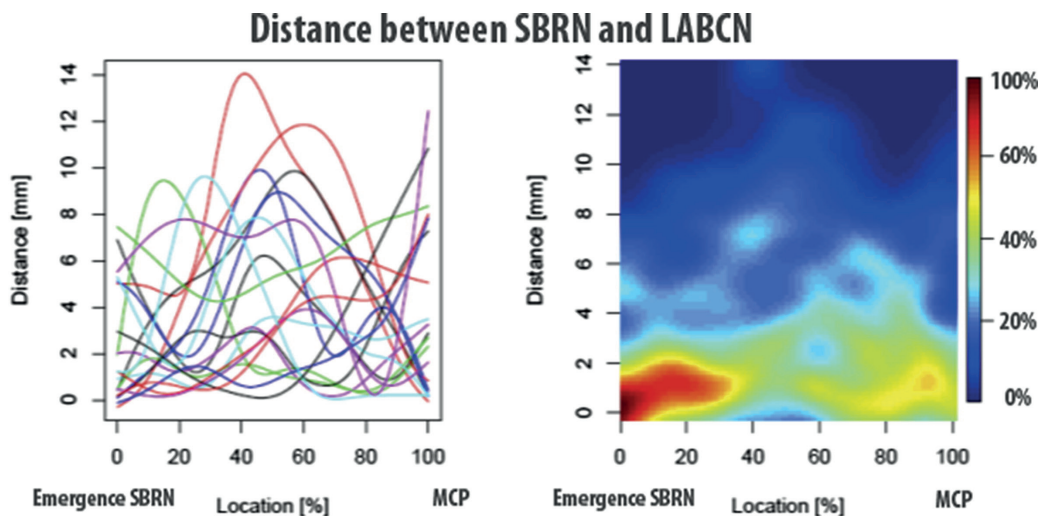


Figure 3. Left: distance of SBRN to LACN in each individual arm. Right: Rendering in which the color indicates the percentage of arms with the distance between the SBRN and LACN being the same. Dark red 100%, dark blue 0%.

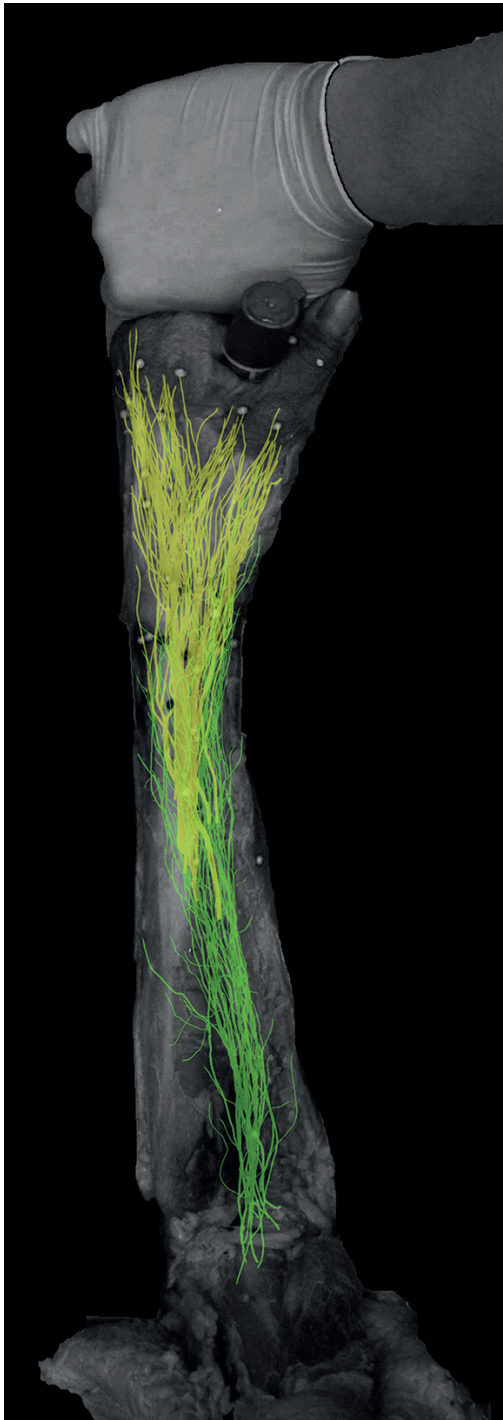


Figure 4. Course of 20 SBRN (yellow) and 20 LACN (green).

In two cases, the most volar branch of the SBRN merged with the LACN continuing along the radial side of the thumb.

In three cases, the LACN merged with the SBRN to innervate the radial aspect of the thumb.

In the images created in CASAM, the close distance between the courses of the two nerves is clearly visible. The image shows that there actually is no real safe zone concerning surgical trauma to LACN and SBRN in the radial part of the wrist ([Figure 4](#)).

DISCUSSION

Surgery to the radial aspect of the wrist is known for its pain-related complications.¹⁶⁻¹⁸ There are many hypotheses to explain the susceptibility of the wrist to neuropathic pain. One of the explanations is based on the intimate anatomical relationship between the end branches of the two nerves. The purpose of this study was to map the course of the LACN and the SBRN and especially the close relation between both nerves at some point resulting in actual, topographical intersections of these two nerves.

In this study, a close relation between the SBRN and the LACN was demonstrated. In all but one arm, the nerves overlapped and intersected on average 2.25 times. The point where the SBRN emerges from a deep point to the BR is also closely related to the first intersection with the LACN. The correlation between the two measurements was high and not dependent on the length of the arm. In 50% of cases, the first crossing was within 18 mm from the point where the SBRN pierces the fascia.

Mackinnon and Dellon² showed that in 75% of cases there is an overlap of the terminal branches of the LACN and SBRN. They concluded that, if the SBRN is damaged, the LACN also has a high probability of being damaged. This lesion of the LACN explains why excision of a neuroma in the SBRN sometimes does not relieve the sensation of pain in patients with neuropathic pain.

Beldner¹⁹ showed that, in several cases, the LACN flanks the cephalic vein on both sides. This study also found a close relation between the cephalic vein and the LACN. This flanking pattern was found in 15% of cases. The fact that the LACN and the cephalic vein are closely related makes it much easier to identify the nerve.

The n demonstrated that the neurosomes of an injured nerve are populated by collateral sprouting fibers from adjacent uninjured nerves.²⁰ These uninjured nerve fibers may change functionally as a consequence of a peripheral nerve lesion.

Due to Wallerian degeneration of the distal segment of the injured nerve, intact nerve fibers are in close proximity of activated Schwann cells, macrophages, and other inflammatory cells, which secrete high levels of neurotrophic factors like NGF. These neurotrophic factors are known to influence excitability, enhance sensory transmission, and/or induce ongoing activity in uninjured peripheral nerve fibers. In addition, in the DRG, signaling from injured DRG cells could infer uninjured DRGs either directly or via nonneuronal cells. The consequences could be changes of excitability and/or ectopic activity in the cell bodies.

Another postulated mechanism for neuropathic pain at the site of the injured nerves is the expression of novel sodium channels that have ongoing and evoked ectopic excitability.

Therefore, it is possible that, if the LACN is sectioned iatrogenically, the SBRN might be responsible for the pain and vice versa. This also explains why, if pain remains after treatment of an SBRN neuroma, it is often diminished on denervation of the LACN, without finding a treatable neuroma in the LACN, as described by LLuch. However, this does not explain the role of the PIN in persistent neuropathic pain on the radial side of the wrist, as this nerve does not have a neurosome in the skin, and yet denervation of the PIN to treat radial-sided pain of the wrist does sometimes reduce pain.

Clinically, when patients present with pain in the area of the SBRN or LACN, diagnostic blockades are performed with 1% lidocaine of SBRN, LACN, PIN, and the palmar cutaneous branch of the median nerve (PCBMN). To determine the efficiencies of such blocks, they are performed in sequential order, with minimally half an hour in between blocks. The next step consists of denervation of the nerve causing pain.

In conclusion, the close (anatomical) relationship between the LACN and the SBRN can be seen as a factor in the explanation of persistent neuropathic pain in patients with traumatic or iatrogenic lesion of the SBRN or the LACN.

ACKNOWLEDGMENTS

The authors would like to thank Y. Steinvoot for her help in providing a room for the dissections. The authors would also like to thank A. Vossen for his help in dissecting and data collection.

REFERENCES

- 1) A.L. Dellon, S.E. Mackinnon. Susceptibility of the superficial sensory branch of the radial nerve to form painful neuromas. *J Hand Surg Br*, 9 (1984), pp. 42–45
- 2) S.E. Mackinnon, A.L. Dellon. The overlap pattern of the lateral antebrachial cutaneous nerve and the superficial branch of the radial nerve. *J Hand Surg Am*, 10 (1985), pp. 522–526
- 3) S.E. Mackinnon, A.L. Dellon. Results of treatment of recurrent dorsoradial wrist neuromas. *Ann Plast Surg*, 19 (1987), pp. 54–61
- 4) A. Truini, G. Cruccu. Pathophysiological mechanisms of neuropathic pain. *Neurol Sci*, 27 (Suppl. 2) (2006), pp. S179–S182
- 5) X.Q. Shu, L.M. Mendell. Neurotrophins and hyperalgesia. *Proc Natl Acad Sci U S A*, 96 (1999), pp. 7693–7696
- 6) P. Anand. Neurotrophic factors and their receptors in human sensory neuropathies. *Prog Brain Res*, 146 (2004), pp. 477–492
- 7) K. Obata, K. Noguchi. BDNF in sensory neurons and chronic pain. *Neurosci Res*, 55 (2006), pp. 1–10
- 8) W. Marcol, K. Kotulska, M. Larysz-Brysz, J.L. Kowalik. BDNF contributes to animal model neuropathic pain after peripheral nerve transection. *Neurosurg Rev*, 30 (2007), pp. 235–243 [discussion 43]
- 9) D. Siniscalco, F. Rossi, S. Maione. Molecular approaches for neuropathic pain treatment. *Curr Med Chem*, 14 (2007), pp. 1783–1787
- 10) D. Siniscalco, C. Giordano, F. Rossi, S. Maione, V. de Novellis. Role of neurotrophins in neuropathic pain. *Curr Neuropharmacol*, 9 (2011), pp. 523–529
- 11) M. Theodosiou, R.A. Rush, X.F. Zhou, et al. Hyperalgesia due to nerve damage: role of nerve growth factor. *Pain*, 81 (1999), pp. 245–255
- 12) R. Heumann, S. Korsching, C. Bandtlow, H. Thoenen. Changes of nerve growth factor synthesis in nonneuronal cells in response to sciatic nerve transection. *J Cell Biol*, 104 (1987), pp. 1623–1631
- 13) A.L. Kerver, L. Carati, P.H. Eilers, et al.. An anatomical study of the ECRL and ECRB: feasibility of developing a preoperative test for evaluating the strength of the individual wrist extensors. *J Plast Reconstr Aesthet Surg*, 66 (2013), pp. 543–550
- 14) A.L. Kerver, A.C. van der Ham, H.P. Theeuwes, et al.. The surgical anatomy of the small saphenous vein and adjacent nerves in relation to endovenous thermal ablation. *J Vasc Surg*, 56 (2012), pp. 181–188
- 15) P.H. Eilers, J.J. Goeman. Enhancing scatterplots with smoothed densities. *Bioinformatics*, 20 (2004), pp. 623–628
- 16) M.S. Arons. de Quervain’s release in working women: a report of failures, complications, and associated diagnoses. *J Hand Surg Am*, 12 (1987), pp. 540–544
- 17) R. Birch, G. Bonney, J. Dowell, J. Hollingdale. Iatrogenic injuries of peripheral nerves. *J Bone Jt Surg Br*, 73 (1991), pp. 280–282
- 18) R.M. McAllister, S.E. Gilbert, J.S. Calder, P.J. Smith. The epidemiology and management of upper limb peripheral nerve injuries in modern practice. *J Hand Surg Br*, 21 (1996), pp. 4–13

- 19) S. Beldner, D.A. Zlotolow, C.P. Melone Jr., A.M. Agnes, M.H. Jones. Anatomy of the lateral antebrachial cutaneous and superficial radial nerves in the forearm: a cadaveric and clinical study. *J Hand Surg Am*, 30 (2005), pp. 1226–1230
- 20) L.S. Duraku, M. Hossaini, B.N. Schuttenhelm, et al.. Re-innervation patterns by peptidergic substance-P, non-peptidergic P2X3, and myelinated NF-200 nerve fibers in epidermis and dermis of rats with neuropathic pain. *Exp Neurol*, 241 (2013), pp. 13–24

